Journal of Hydrology: Regional Studies 12 (2017) 396–412

Contents lists available at ScienceDirect

Journal of Hydrology: Regional Studies

journal homepage: www.elsevier.com/locate/ejrh

Capability of meteorological drought indices for detecting soil moisture droughts

Devanmini Halwatura[a,*], Neil McIntyre[a], Alex M. Lechner[a,b], Sven Arnold[a]

[a] Centre for Water in the Minerals Industry, Sustainable Mineral Institute, The University of Queensland, Australia
[b] School of Environmental and Geographical Sciences, University of Nottingham, Malaysia Campus, Semenyih, Malaysia

ARTICLE INFO

Keywords:
Hydrus-1D
Soil water pressure
Standardized Precipitation Index
Reconnaissance Drought Index
Drought

ABSTRACT

Study region: Eastern Australia
Study focus: Long-term monitoring of soil moisture is a time- and cost-intensive challenge. Therefore, meteorological drought indices are commonly used proxies of periods of significant soil moisture deficit. However, the question remains whether soil moisture droughts can be adequately characterised using meteorological variables such as rainfall and potential evaporation, or whether a more physically based approach is required. We applied two commonly used drought indices – the Standardized Precipitation Index and the Reconnaissance Drought Index – to evaluate their performance against soil moisture droughts simulated with the numerical soil water model Hydrus-1D. The performance of the two indices was measured in terms of their correlation with the standardised simulated monthly minimum soil water pressures, and their capability to detect soil moisture droughts that are potentially critical for plant water stress.
New hydrological insights for the region: For three typical soil types and climate zones in Eastern Australia, and for two soil profiles, we have found a significant correlation between the indices and soil moisture droughts detected by Hydrus-1D. The failure rates and false alarm rates for detecting the simulated soil moisture droughts were generally below 50% for both indices and both soil profiles (the Reconnaissance Drought Index at Melbourne was the only exception). However, the complexity of Hydrus-1D and the uncertainty associated with the available, regionalised soil water retention curves encourage using the indices over Hydrus-1D in absence of appropriate soil moisture monitoring data.

1. Introduction

Drought is one of the most complex, harmful and least understood type of climatic event, causing an annual average of 6–8 billion USD of damage globally (Edwards, 1997; Keyantash and Dracup, 2002; Saghafian et al., 2003; Yagci et al., 2013); and it is expected that the severity and frequency of droughts will change in the future due to climate change (Dai, 2012; McCarthy, 2001; Van Loon et al., 2016). Droughts are classified into meteorological, agricultural, hydrological, and socioeconomic droughts (Passioura, 2007; Shiau et al., 2012; Zargar et al., 2011). Across these drought classes over 150 drought indices exist and are widely accepted as measures for monitoring of spatial and temporal variability of water shortage (Quiring, 2009; Zargar et al., 2011). Depending on the climatic region, the type of drought and the purpose of a study, drought indices use information on rainfall, potential evaporation, soil moisture, surface water, groundwater or supply shortages (American Meteorological Society, 1997; Hao and AghaKouchak, 2013; Khedun et al., 2012). Often, measures of the severity and duration of droughts are derived from these indices (United States Drought

* Corresponding author.
E-mail address: d.halwatura@uq.edu.au (D. Halwatura).

http://dx.doi.org/10.1016/j.ejrh.2017.06.001
Received 11 January 2017; Received in revised form 25 May 2017; Accepted 6 June 2017
Available online 27 July 2017
2214-5818/ © 2017 The Authors. Published by Elsevier B.V. This is an open access article under the CC BY-NC-ND license (http://creativecommons.org/licenses/BY-NC-ND/4.0/).

Monitor, 2017) and drought frequency analysis is used to estimate the return period or exceedance probability of a drought of given severity and/or duration (Halwatura et al., 2015a; Kwak et al., 2015; She et al., 2016).

Droughts play a critical role in agriculture and ecosystem restoration (Carrick and Krüger, 2007), as soil moisture is the key control on many biogeochemical processes in the water, carbon, or nitrogen cycle. The movement of water from soil pores to plant roots and leaves follows potential energy gradients that are predominantly determined by the soil moisture balance (Prentice et al., 1992; Rodriguez-Iturbe, 2000). If soil moisture is depleted, gradients in the soil water potential gradually break down, thereby affecting vegetation negatively such as reducing crop production or failing ecosystem establishment (National Drought Mitigation Center, 2013). Soil moisture droughts can be defined as shortage of soil moisture that causes permanent damage or failure of vegetation (Cammalleri et al., 2016) (here and throughout the paper we prefer the term 'soil moisture drought' to 'agricultural drought' because the results have relevance beyond agricultural applications, e.g. Boken et al., 2005; Woli et al., 2012). Soil moisture drought indices such as the Palmer Drought Severity Index (Palmer, 1965), Crop Moisture Index (Palmer, 1969), and Z index (Palmer, 1968) account for the water needs of plants and integrate soil moisture data. Recently developed indices incorporating soil moisture include the Drought Severity Index (Cammalleri et al., 2016) and the Soil Water Deficit Index (Martínez-Fernández et al., 2005; Martínez-Fernández et al., 2015). However, practical application of these indices is challenging as long-term soil moisture data are rarely available and the establishment of soil moisture monitoring systems is expensive and time consuming (Wilson et al., 2016; Zawadzki and Kędzior, 2016). Therefore, simpler drought indices such as the Standardized Precipitation Index (SPI) and Reconnaissance Drought Index (RDI) are often used when the necessary quality and quantity of observed soil moisture data are not available (Halwatura et al., 2015b; Wang et al., 2015).

Alternatively, physically based soil water models can be used to simulate soil water content, fluxes and pressures (Anderson et al., 2012; Granier et al., 1999; Hao and AghaKouchak, 2013). Together with local soil properties, long-term meteorological data (and potentially irrigation) can be used as inputs to estimate the probability of critical thresholds of soil water pressure being exceeded (such as the wilting point). Selecting a threshold is a complicated, as well as a critical, step, because plant related soil moisture levels are rarely found in literature. However, the application of physically based models for soil moisture drought estimation is challenging due to a range of issues such as uncertainty associated with the data and approximations of biophysical processes (Chowdhary and Singh, 2010; Li et al., 2005; Mishra and Singh, 2011; Wang et al., 2011). Some studies have addressed these issues by comparing soil moisture observations with meteorological drought indices (Wang et al., 2015; Wang et al., 2016). However, these methods are limited to short periods with a small sample size of observations or are validated against long-term soil moisture data derived from climate model simulations rather than empirical monitoring data (Cammalleri et al., 2016). In this regard, the following are still unclear: (1) under what conditions simple meteorological drought indices can potentially replace more complex modelling approaches to assess soil moisture droughts, and what values of the indices correspond to critical thresholds in soil moisture contents and hence define a drought occurrence; and (2) what relative reliability is achieved from using a physically based soil moisture model rather than drought indices to detect drought occurrences, considering the inherent uncertainty in the model? These questions apply to estimating drought under both historical and predicted meteorological conditions.

Therefore, the objective of this paper is to evaluate the capability of simple meteorological drought indices to estimate the severity and duration of soil moisture deficits that have been synthesised using a physically based soil water model. Our analysis is based on climate and soil hydraulic data from across three distinct sites in Eastern Australia.

2. Analysis

Our analysis involved the following five steps (Fig. 1):

1. Selection of representative sites typical for Eastern Australia with comprehensive availability of climate data (rainfall, potential evaporation) and soil hydraulic data (soil water retention curve).
2. Selection of suitable meteorological drought indices (SPI, RDI) and their calculation using time series of observed climate data, and estimation of corresponding time series of soil water pressure using a physically based soil water model (Hydrus-1D).
3. Performance evaluation of the drought indices against the standardised simulated soil water pressure values. This includes identifying thresholds that define drought occurrence; and the design, evaluation and analysis of metrics of characterising how well the indices represent the physically based soil water pressure.
4. Analysis of the sensitivity of simulated soil water pressure to uncertainty in the soil hydraulic parameters (water retention curves).
5. Analysis of the effect of that uncertainty in the physically based soil water model affecting the comparison with the drought indices.

Step 1. Selection of representative site across Eastern Australia

The availability of comprehensive (i.e., high coverage) long-term rainfall and potential evaporation data is crucial for the assessment of water shortage periods in relation to the long-term average. For the three selected sites, Cairns, Bourke and Melbourne, historic daily rainfall and potential evaporation point data (calculated using the Penman-Monteith equation) were available for 25 years within the period 1971–2013 (Table 1) (Bureau of Meteorology, 2013). Based on the metadata for these sites (Bureau of Meteorology, 2013), the data quality is considered good. During the periods shown in Table 1, the data were more than 97% complete. Missing periods were infilled using the nearest gauge in the Bureau of Meteorology database for which corresponding data were available. These periods could not be omitted as drought index estimations and the Hydrus-1D model requires continuous-time inputs, and the corresponding period that might be neglected in model evaluation is not obvious. Therefore it is assumed that the

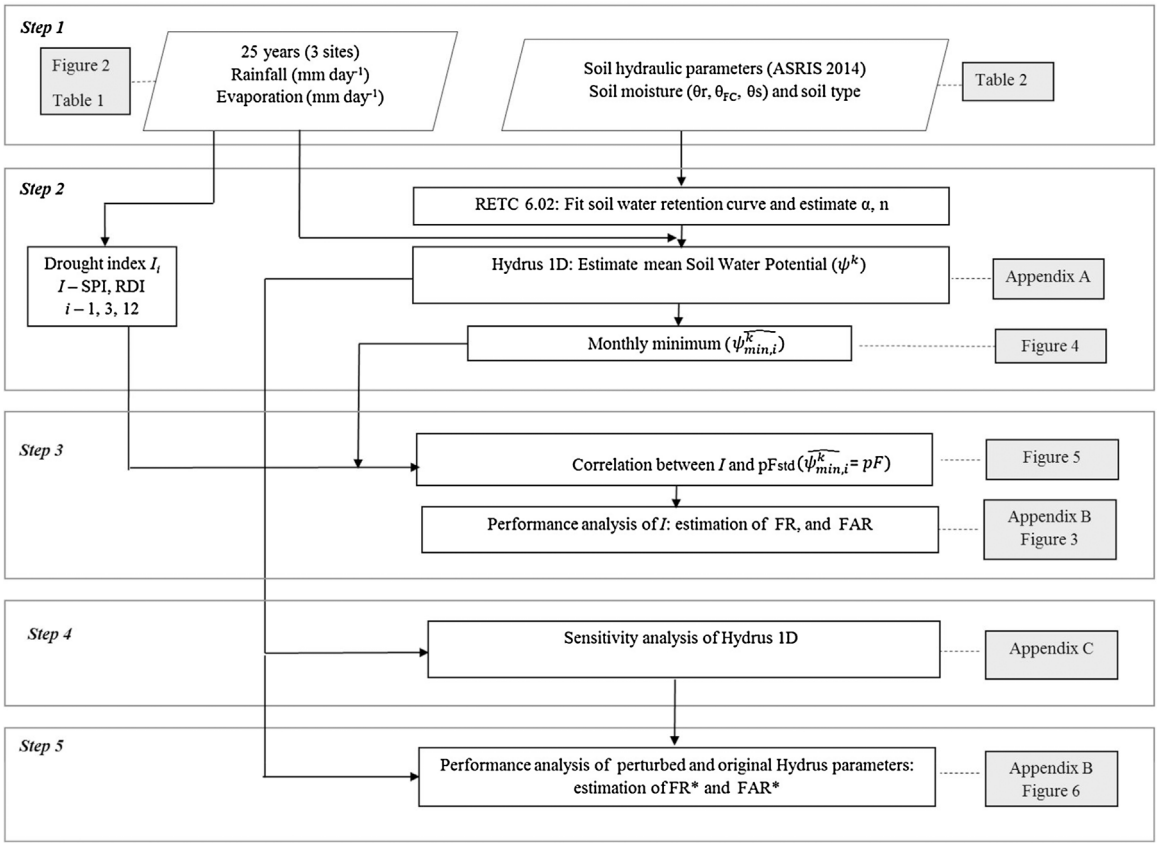

Fig. 1. Schematic diagram of steps applied in the methodology. See Section 2 for further details. Step 1: Selection of three sites representing typical climates in Eastern Australia. Step 2: Estimation of drought indices and simulation of standardised soil water pressure. Step 3: Evaluation of the drought indices against standardised minimum soil water pressures. Step 4: Sensitivity analysis of simulated soil water pressure. Step 5: The effect of uncertainty on the relative value of the physically based soil water model.

Table 1
Climate indices for selected locations with focus on rainfall R (subscripts w and s denote winter and summer, respectively) and potential evaporation PET.

Location	Length of meteorological data (years)	Climate index		Köppen-Geiger[c] climate classification
		R/PET[a]	R_w/R_s[b]	
Cairns (−17.457 S, 145.992 E)	1988–2013 (25)	0.91	0.10	Tropical, savannah
Melbourne (−37.966 S, 144.553 E)	1988–2013 (25)	0.51	0.95	Temperate, without dry season
Bourke (−30.233 S, 145.917 E)	1967–1992 (25)	0.20	0.61	Arid, steppe

[a] (UNEP, 1992).
[b] Based on average of three-months of rainfall during winter (June–August) and summer (December–February).
[c] (Peel et al., 2007).

Table 2
Soil type and water retention parameters of selected sites and the ranges used for the sensitivity analysis.

Soil parameter Soil type	Cairns Sandy loam	Melbourne Sandy loam	Bourke Sandy clay loam
θ_r ($cm^3\ cm^{-3}$)	0.05 (0.025–0.06)	0.1(0.05–0.15)	0.07 (0.035–0.105)
θ_s ($cm^3\ cm^{-3}$)	0.47 (0.235–0.705)	0.513 (0.025–0.769)	0.33 (0.165–0.495)
α (cm^{-1})	0.1864 (0.093–0.279)	0.1114 (0.055–0.167)	0.023 (0.012–0.034)
n (−)	1.2087 (1.087–1.813)	1.3695 (1.232–2.05)	1.296 (1.166–1.944)
k_s (cm day^{-1})	106.1	106.1	31.44

α: First-order mass transfer coefficient, n: curve shape parameter, θ_s: soil water content at saturation, θ_r: residual water content, K_s: saturated hydraulic conductivity.

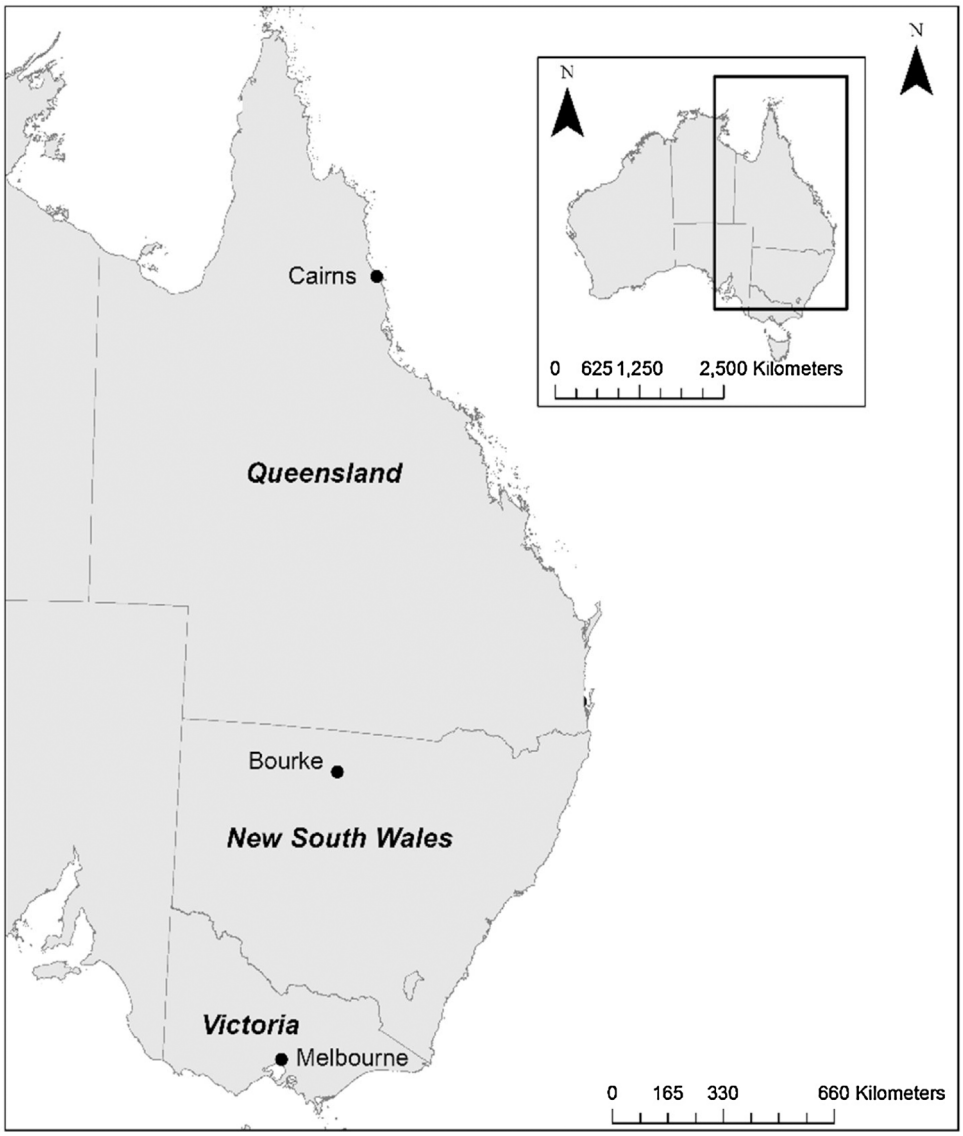

Fig. 2. Selected locations of interest.

infilling will not unduly influence the evaluations in Steps 3 to 5. Likewise, soil hydraulic data were available to derive the water retention curves of the predominantly Sandy Loam soils in Melbourne and Cairns and Sandy Clay Loam soils in Bourke (Australian Soil Resource Information System, 2011) (Table 2). While soils are variable in these regions, only these dominant soil types were considered for this study. Apart from the sufficient availability of climate and soil data, these three sites were chosen as they cover the three main climatic regions across Eastern Australia – tropical, arid and temperate in Cairns, Bourke and Melbourne, respectively (Halwatura et al., 2015a; Köppen, 1936) (Table 1, Fig. 2).

Step 2. Estimation of drought indices and soil water pressure

This step generated data for two drought indices and the simulated soil water pressure data. The SPI and RDI drought indices were selected based on simplicity of the calculation process, the modest data requirements and their perceived widespread suitability. SPI is one of the most commonly used indices including a wide range of application types (e.g. Hao et al., 2016); however many comparative studies have preferred RDI for estimating extreme droughts where potential evaporation is considered important (Asadi Zarch et al., 2015; Jamshidi et al., 2011; Khalili et al., 2011; Shokoohi and Morovati, 2015). Recent studies recommend SPI and RDI for assessing droughts in temperate, arid and tropical climates; and that they may perform well relative to data from remote sensing methods, climate models, and more complex drought indices (Elkollaly et al., 2017; Kostopoulou et al., 2017; Ma'rufah et al., 2017; Zarei et al., 2016; Zhang et al., 2017). In context of Australian climates, SPI and RDI have been frequently used for comparative drought assessments, for example (Barua et al., 2009; Halwatura et al., 2015a; Halwatura et al., 2016; Kirono et al., 2011; Rahmat et al., 2015).

Both indices were calculated using climate inputs averaged over one, three and twelve-month time periods. In contrast to other

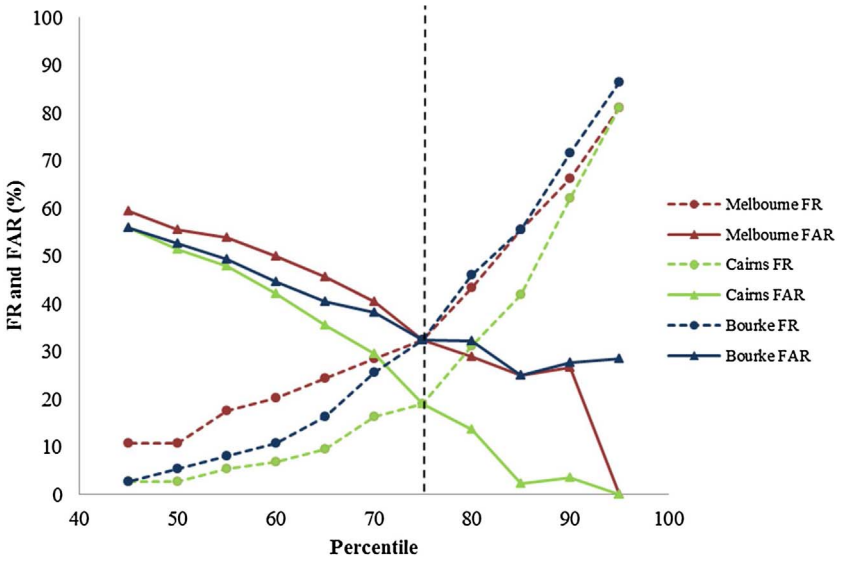

Fig. 3. The change of FR and FAR in relation to the selected threshold percentile for the SPI for a 30 cm soil profile. Dotted line indicates the 75th percentile used in the study.

studies (e.g. Martínez-Fernández et al., 2015; Wang et al., 2015; Wang et al., 2016), which standardise SPI and RDI using the long-term season-specific averages, the indices were standardised using the long-term (25-year) annual averages (Eqs. (1) and (2a) (2b)), thereby the time-series of standardised indices exhibit seasonal patterns (Fig. 4). The SPI was derived by fitting the rainfall records to a probability distribution and transforming it into a normal distribution with zero mean and unit standard deviation. Rainfall conditions greater or smaller than average rainfall are represented by positive or negative values of SPI respectively (McKee et al., 1993; Shiau et al., 2012). Following McKee et al. (1993), using the three-month time-scale as an example, SPI was calculated for each site as,

$$SPI_i = \Phi^{-1}\left(F_R \frac{(r_{i-2} + r_{i-1} + r_i)}{3}\right) \tag{1}$$

where r is the rainfall, F_R is the non-exceedance probability of the three-month average value, calculated by fitting a Gamma distribution using the method of moments, the subscript i is the month number ranging from the third to the last month in the record, and Φ^{-1} is the inverse cumulative distribution function of the standard normal distribution.

The standardised three-monthly RDI (Tsakiris and Vangelis, 2005) was calculated for each site as:

$$RDI_i = \frac{\ln(\gamma_i) - \mu_{\ln(\gamma)}}{\sigma_{\ln(\gamma)}}, \tag{2a}$$

with

$$\gamma_i = \frac{P_{i-2} + P_{i-1} + P_i}{PET_{i-2} + PET_{i-1} + PET_i} \tag{2b}$$

where P and PET are rainfall and potential evaporation respectively, i is the month number ranging from the third to the last month in the record, and $\mu_{\ln(\gamma)}$and $\sigma_{\ln(\gamma)}$ are the arithmetic mean and standard deviation of$\ln(\gamma)$ over all its values for that site.

For the derivation of soil water pressure using the physically based soil water model (in addition to the climate data) water pressure characteristics of the soils were provided by the Australian Soil Resource Information System (2011). These data included the soil moisture content and water pressure at saturation (0 hPa), field capacity (−100 to −330 hPa), permanent wilting point (−15,000 hPa) and air-dry conditions (−1,000,000 hPa). The water retention curve was fitted to these data using RETC 6.02 (Van Genuchten et al., 1991) to estimate the first-order mass transfer coefficient α and curve shape parameter n. These two parameters were used, together with the soil water content at saturation (θ_s), the residual water content (θ_r) and the saturated hydraulic conductivity (K_s) (Table 2), to simulate one-dimensional water flow in Hydrus-1D (Šimůnek et al., 2008) and to estimate daily soil water pressure (ψ). We selected Hydrus-1D as physically based model because of its free availability (ensuring reproducibility) and its well-established acceptance in the soil science community (Šimůnek et al., 2016). We used the same daily rainfall and potential evaporation inputs as those used to calculate the drought indices. The lower boundary condition at 1 m depth was set as free drainage and the upper boundary condition was set as atmospheric with surface runoff (Appendix A).

The primary assumptions of the soil water modelling were that (i) the soil water characteristics (Australian Soil Resource Information System, 2011) were representative of the selected soil types, including incorporating local vertical and lateral heterogeneities, (ii) using the effective parameter values of the water retention curve, Richards' equation is an adequate approximation of

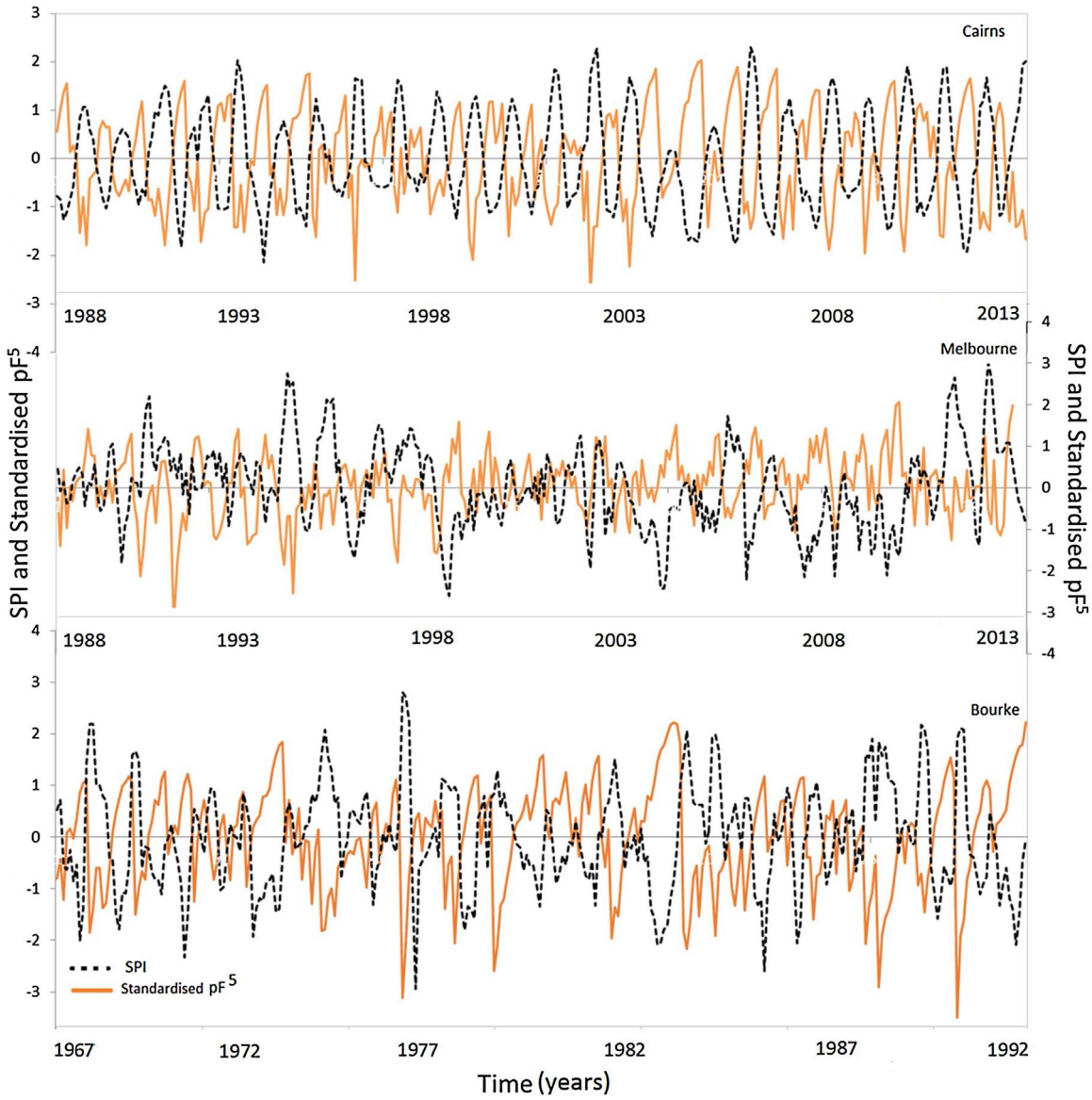

Fig. 4. Time series of the simulated standardised monthly minimum soil water pressure over 5 cm depth and the SPI for the three selected studies sites.

the unimodal soil permeability, (iii) the free drainage lower boundary condition is an adequate approximation of the local conditions, (iv) the evaporative demand primarily determines the upper boundary condition, (v) sub-daily variations in soil water pressure are insignificant and the use of daily averaged input and output data is sufficient, and (vi) there is no irrigation so that drought is not influenced by any groundwater or surface water storages. No in-situ measurements were used to calibrate and test the Hydrus-1D model, therefore the results from Step 3 represent the hypothetical, regionally representative soils described by the parameters in Australian Soil Resource Information System (2011), rather than being site-specific. The ability of Hydrus-ID to represent soil water content and pressure dynamics using regionalised parameter estimates is supported by a large number of previous assessments including for relevant soil types and climates (Chen et al., 2014). For example, for temperate climates with dominant loam soil and sandy soils Hydrus have been recommended as reasonable methods to estimate soil moisture for shallow soils (< 40 cm) (Hollander et al., 2016; Kato et al., 2010). Also for temperate climates, Pan et al. (2011) concluded that they successfully simulated soil moisture for sandy loam soil in 25 cm and 100 cm depths. For tropical climates with dominant clay soils Hydrus-1D was considered to have estimated soil moisture with reasonable accuracy in absence of any ground-based measurements (Gupta et al., 2014). For cold climates simulated soil moisture data provided significant correlations for shallow soils (< 30 cm) (Naylor et al., 2016; Schwarzel et al., 2006). Further Zhu et al. (2009) considered that Hydrus-1D was successful in arid climates (with sandy soil) with extended droughts to study groundwater movement into the root zone (Zhu et al., 2009). Further, Dasgupta et al. (2015) used Hydrus-1D to simulate soil water potential in drought conditions to study the water stress and yield of rice varieties. We recognise that this overview of relevant applications of Hydrus-ID does not permit the conclusion that the model is accurate for any particular soil type

and application in the case study regions; rather we conclude that it is not an unreasonable way to manufacture a regionally-representative soil moisture response for drought analysis. The fitness for purpose for application to a specific site is addressed through the uncertainty analysis in Step 4.

Step 3. Evaluation of the drought indices against soil water pressure

For each site and each month, we extracted the monthly minimum soil water pressure (hPa) averaged from the soil surface to 5 cm depth ($\hat{\psi}^{5}_{min,i}$), and also from the soil surface to 30 cm depth ($\hat{\psi}^{30}_{min,i}$). While we considered the shallow soil represented by the 0–5 cm depth range to be critical for plant establishment such as seedling emergence, the deeper soil represented by the 0–30 cm depth range was considered to be critical for the persistence of most annual plants (Martínez-Fernández et al., 2015). We used the minimum monthly soil water pressure as the reference value for potential plant water stress assuming that one incidence of exceeding a species-specific water pressure threshold causes irreversible plant water stress (Blum, 2011; Tezara et al., 1999), which is more biologically relevant than monthly averaged values, for example monthly averaged values that do not reflect the short-term variability of soil moisture dynamics

We then transformed soil water pressure into logarithmic values and standardised them using a standard normal distribution (pF_{std}) (Carrão et al., 2016; Kumar et al., 2016):

$$pF_{std}{}^{5} = \log_{std}(-\hat{\psi}^{5}_{min,t}), \tag{3a}$$

$$pF_{std}{}^{30} = \log_{std}(-\hat{\psi}^{30}_{min,t}), \tag{3b}$$

and evaluated the correlations between simulated soil water pressure (Eq. (3a), (3b)) and the drought indices (SPI_i, RDI_i). We also evaluated the correlations between $pF_{std}{}^{5}$ and $pF_{sdt}{}^{30}$ and SPI_{i-1} and RDI_{i-1} in case the three month averages defined in equation (1), (2a) and (2b) more strongly influenced the next month's minimum soil water pressure.

We calculated the failure rate (FR) and false alarm rate (FAR) to quantify the success of the drought indices in detecting critical periods of lacking soil water availability based on the simulated low soil water pressure events (See Appendix B Fig. B1 for further explanation):

$$FR = \frac{\#E(a)}{\#E(a+ b)} \tag{4}$$

where #E(a) is the number of simulated low soil water pressure events not detected by the drought index, and #E(a + b) is the total number of simulated low soil water pressure events.

Likewise, the FAR was calculated as:

$$FAR = \frac{\#E(c)}{\#E(b+ c)} \tag{5}$$

where #E(c) is the number of drought events detected by the drought index not corresponding to periods of low simulated soil water pressure, and #E(b + c) is the total number of droughts detected by the drought index. The lower the FR and FAR values, the more capable the drought index is in detecting periods of low soil water pressure.

Ideally, the threshold determining a low simulated soil water pressure would be physically based; however, commonly used physically based thresholds, such as the wilting point, do not necessarily coincide with stress levels of plant communities and in most cases plant available thresholds are not available (Bond and Kavanagh, 1999; Wonkka et al., 2016). Likewise, commonly used drought classifications are arbitrary and the use of percentiles has been suggested instead (Agnew, 2000; Mueller and Zhang, 2016; Svoboda et al., 2002). Therefore, instead of a physically based threshold of soil water pressure, we chose the value that gave the overall lowest values of FR and FAR, which was the 75th percentile representing the upper limit of potential performance; and for consistency, the 75th percentile of the estimated drought indices was used to define a drought event (Fig. 3).

Step 4. Sensitivity analysis of simulated soil water pressure

In this step we explored the effect of uncertainties in the water retention curve parameters on the simulated soil water pressure. We assessed the local sensitivity (Oakley and O'Hagan, 2004) of the simulated soil water pressure to uncertainty in θ_r, θ_s, α, and n. The normalised relative sensitivity S was calculated for each site as

$$S = \frac{d\hat{\psi}^{k}_{min} / \hat{\psi}^{k}_{min}{}^{0}}{dP_{WRC}/P^{0}_{WRC}} \tag{6}$$

where $\hat{\psi}^{k}_{min}$ is the simulated monthly minimum soil water pressure in depth k, P_{WRC} refers to one of the four parameters in the soil water retention curve, the superscript 0 refers to the initial reference values of $\hat{\psi}^{k}_{min}$ and P_{WRC}, respectively, and d refers to the difference between the perturbed and reference values. Each of the four parameters was varied in turn, between values $dP_{WRC}/P^{0}_{WRC} = [-0.5, 0, +0.5]$ using ± 10% intervals, while all other parameters were kept at default values (Table 2). The simulated mean soil water pressure was considered sensitive to uncertainty in the soil hydraulic model if $S > 1$.

Step 5. The effect of uncertainty on the relative value of the physically based soil water model

In the final step we conducted a local sensitivity analysis in order to assess the effect of uncertainties in the hydraulic model parameters on FR and FAR (Appendix B Fig. B2). Using this method we explored how well we would expect the hydraulic model to detect drought events given scenarios of hydraulic model uncertainty. We used simulated soil water pressure (ψ_{min}^{k}) based on the default parameters of the water retention curves (Table 2) as a benchmark representing the 'true' soil water pressure response. This was compared against the simulated soil water pressure based on the hydraulic model parameter perturbations that caused the highest and median values of S (bold and italic in Appendix C).

Then we calculated FR* and FAR* as:

$$FR^* = \frac{\#E(a^*)}{\#E(a^* + b^*)} \tag{7}$$

and

$$FAR^* = \frac{\#E(c^*)}{\#E(b^* + c^*)} \tag{8}$$

where $\#E(a^*)$ is the number of low soil water pressure events simulated with the default water retention curve but not simulated with the perturbed water retention curve, $\#E(a^* + b^*)$ is the total number of low soil pressure events simulated with the default water retention curve, $\#E(c^*)$ is the number of low soil pressure events simulated with the perturbed water retention curve but not simulated with the default water retention curve, and $\#E(b^* + c^*)$ is the total number of low soil pressure events simulated with the perturbed water retention curve.

If FR* > FR or FAR* > FAR, the assumed parameter uncertainty in the hydraulic model critically affects its relative ability to detect droughts, so that the simple drought index may be preferred over the more complex soil water model, even if FR or FAR is high.

3. Results

Out of the three alternative time-scales used to define SPI and RDI, we found that the three-month time-scale gave the highest correlations with standardised soil water pressure for all locations and soil profiles. For the sake of simplicity we only present the results of three-month time-scale and provide the results for the one-month and twelve-month time scales in Appendix D. Fig. 4 shows the time-series of results for the three-month SPI and pF_{std}^{5}. The most severe drought in the 25-year period at Bourke occurred in the months April-June in 1976 with SPI = −2.94 and a corresponding soil water pressure in the deeper soil, $pF_{std}^{5} = 0.5$ and $pF_{std}^{30} = 2.4$. These three months had a total rainfall of 2.6 mm compared with the average rainfall in these three months of 30.7 mm, and similar values were obtained for the severest droughts in Melbourne and Cairns (respectively, SPI = −2.57, $pF_{std}^{5} = 1.5$ and $pF_{std}^{30} = 2.2$; and SPI = −2.1, $pF_{std}^{5} = 1.8$ and $pF_{std}^{30} = 1.9$).

Both drought indices were significantly correlated ($p < 0.05$) with the standardised soil water pressure, but the correlation was stronger for the deeper (30 cm) soil profiles (Fig. 5). The correlations were strongest for tropical Cairns ($R^2 = 0.69$) and arid Bourke ($R^2 = 0.51$) for the SPI and RDI, respectively. The lowest correlations were observed in Melbourne at both drought indices and each soil profile (Fig. 5). Because soil water pressure may take some time to respond to meteorological changes, we re-calculated the correlations after lagging the timeseries of the soil water pressure behind the time-series of the drought index. Using a lag of one month, so that the minimum pFstd in month i corresponds to SPIi-1 calculated using equation (1), correlations between standardised soil water pressure values and drought index values were lower than those listed above. Therefore there is no evidence of a lag between SPI or RDI and soil water pressure minima that is not captured within Eqs. (1) and (2a), (2b).

Because the 75th percentile was used to define the drought index as well as the soil water pressure thresholds, in this case E(a) = E(c) and E(a + b) = E(b + c), therefore FR = FAR. Hence only FR is referred to here. The SPI performed better than the RDI in terms of FR across all locations and soil profiles, except for the 5 cm soil profile at Bourke. FR using the SPI ranged between 19% and 42%, and the values using the RDI ranged between 36% and 68% (Table 3). Using the RDI, the FR values were always higher for the deeper soil profiles, while for the SPI they were lower except for tropical Cairns where the FR was the same for both profile depths. In temperate Melbourne, the FR values derived using RDI were higher than for other locations (58% and 68% for the two soil profiles), while results for tropical Cairns showed the greatest improvement moving from the RDI to the SPI (e.g. FR reduced from 46% to 19% for the 30 cm soil profile).

Varying the SPI and RDI threshold values, while maintaining the 75% threshold applied to the simulated soil water pressures, illustrates the sensitivity to the arbitrary choice of threshold (Fig. 3). As expected, when the SPI threshold increased (i.e., only extreme values of the SPI are classed as droughts), FR became high and FAR became low. For example, using the 95th percentile, FAR values for Cairns and Melbourne approached zero and FR values approached 81%. Although there may be particular circumstances when low FR or FAR rates may be the aim, the results confirm that a balanced performance is achieved by calibrating the actual number of drought events (in this case represented by the simulation) so that it is equal to the modelled number of drought events (in this case using the SPI and RDI).

The results of the Hydrus-1D parameter sensitivity analysis are shown in Appendix C. The simulated soil water pressure was most sensitive to uncertainty in parameters of the water retention curve in tropical Cairns, where the relative sensitivity ranged from 1.4 (when perturbing parameter n) to 4.0 (when perturbing parameter θ_s). In other words, the simulated soil water pressure rose by up to

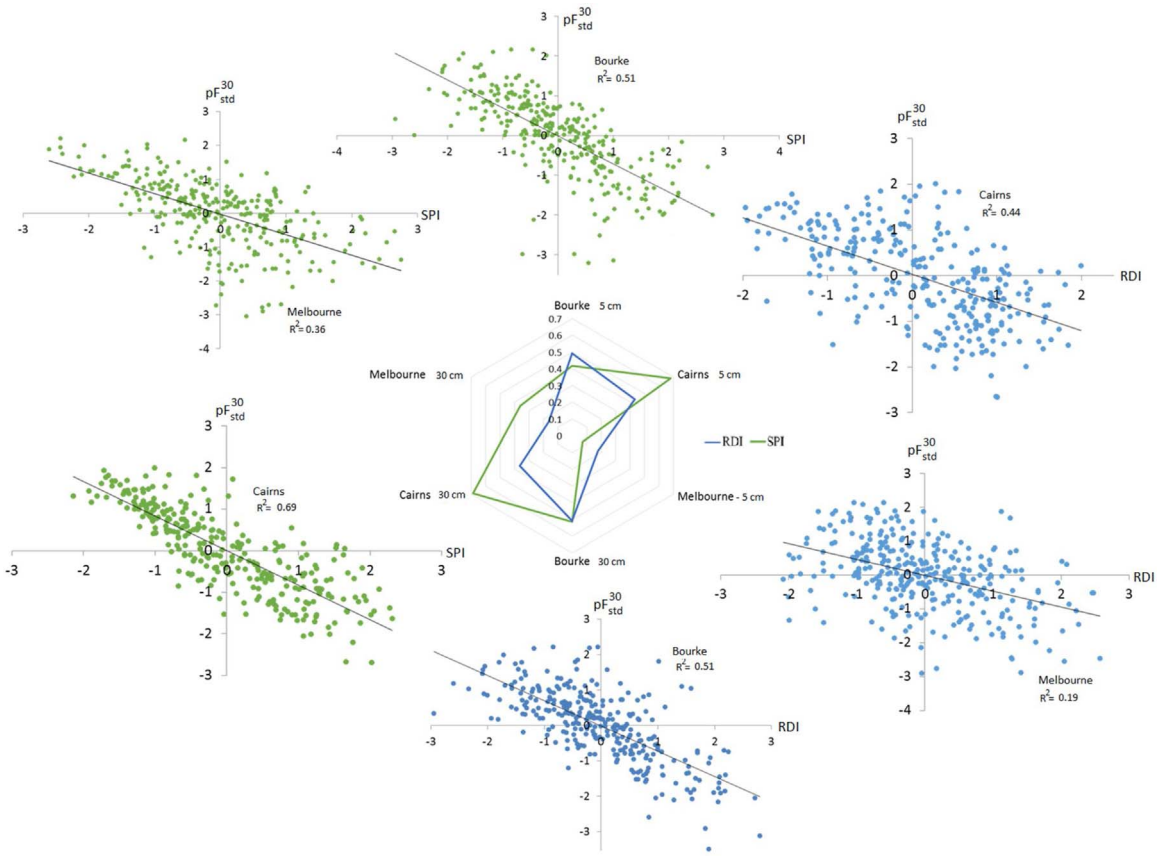

Fig. 5. Web plot of correlations between standardised simulated monthly minimum soil water pressure pF_{std} and the SPI (green) and RDI (blue) for 5 cm and 30 cm soil profile, respectively (centre). The scatter plots show the pressure data for only the 30 cm soil profile, which gave the higher correlations in all cases.

Table 3
Performance analysis of drought indices based on standardised monthly minimum soil water pressure for the threshold value of 75th percentile.

Location	Soil profile (cm)	Drought index	
		FR (%)	
		RDI	SPI
Cairns	5	45	19
	30	46	19
Melbourne	5	58	41
	30	68	32
Bourke	5	36	42
	30	41	32

Note: FAR values are identical to FR values.

4% after changing the default parameter values by 1%. In contrast, the highest sensitivities across the other locations ranged from 0.3 in temperate Melbourne to 2.7 in arid Bourke. Examples of time series of monthly minimum soil water pressure in the 0–5 cm depth range for Bourke using default and perturbed parameter α are shown in Appendix E.

The performance of the SPI in detecting soil moisture droughts relative to the perturbed Hydrus-1D is presented in Fig. 6 by showing the differences between FR*–FR (the values of FAR*–FAR are identical). The results in Fig. 6 show that for all locations the errors introduced by the assumed uncertainty in the water retention curves are greater than those introduced by the use of SPI. Generally, the simulation model performed relatively well for shallow soils than for deeper soil profiles (Fig. 6).

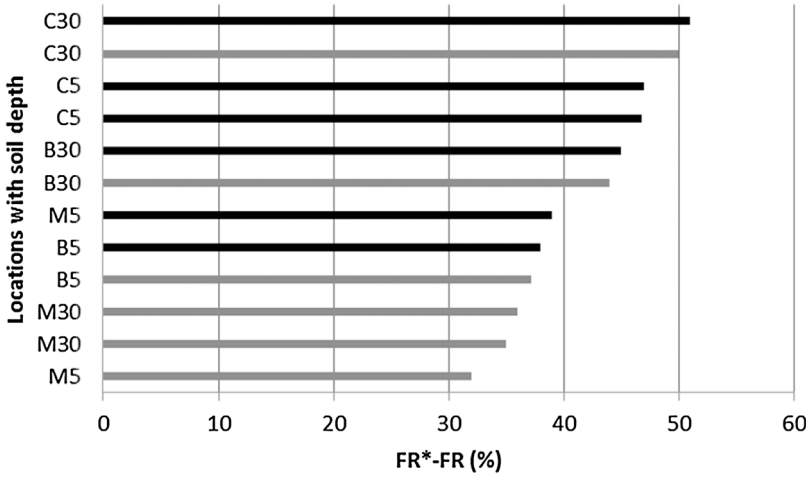

Fig. 6. The difference between the FR*–FR for all sites and soil profiles for SPI. The positive values indicate that drought indices are more reliable than the hydraulic model due to the uncertainties of the model. Black and grey bars indicate the highest sensitive and median sensitive values of perturbed model respectively. Values of FAR*–FAR are the same as FR*–FR. FR* represents the mean of three assessed parameters (θr, θs, α). B: Bourke, C: Cairns, M: Melbourne.

4. Discussion

In this study we assessed the capability of selected meteorological drought indices to identify periods of soil water drought through a comparison with the physically based soil water model, Hydrus-1D. We used soil hydraulic properties and 25 years of climate data from three locations in eastern Australia representing tropical, temperate and arid climates. We analysed the correlations between the indices and standardised simulated soil water pressures, and the frequency with which the indices detected soil water pressure thresholds being passed. The relative capabilities of the indices and the soil water model, considering scenarios of uncertainty in the latter, were also assessed. The drought indices have variable success in detecting the periods of limited soil water availability. The frequency which the drought indices failed to detect periods of soil water deficit and the frequency with which they falsely detected periods of soil water deficit (FR and FAR respectively) are generally below 50% (in all cases except at Melbourne using the RDI) and as low as 19% (at Cairns using the SPI) (Table 3). Due to the uncertainties in the simulation model parameters, which (assuming the default Hydrus-1D model is a reasonable reference point) represent the level of uncertainty that may occur in a practical application, the drought indices are considered generally more reliable indicators of plant water stress due to drought (Fig. 6). This highlights the importance of precise estimation of the soil water retention curve. Although our results show a strong preference for using the simpler index (SPI), it is reasonable to also conclude that, when and where adequately supported by data and modelling expertise, a physically based soil water model should be used in preference.

One of the major concerns of using meteorological drought indices is false prediction of soil moisture drought or over-estimation of its frequency (Sheffield et al., 2012; Törnros and Menzel, 2014; Touchan et al., 2005). For example, the Palmer Drought Severity Index has overestimated global drought severity over the past 60 years (Sheffield et al., 2012). Also tree growth assessments showed that the SPI tends to overestimate tree ring index values (Touchan et al., 2005). Our results were 'calibrated' to achieve a balance between over-estimation (high FAR values) and under-estimation (high FR values) (Fig. 3), yet at best achieved FR and FAR values of 19%. There are several potential reasons why the performance was not better, including the simplicity of the indices used, the disparity of time-scales and the potential errors in the simulated soil water data. These are expanded upon below.

Rainfall and potential evaporation are treated simplistically in the calculation of the SPI and RDI (Shiau, 2006). Eqs. (1) and (2a), (2b) contain combinations of the climate variables that give convenient and intuitive indices of drought (Shiau and Modarres, 2009; Vangelis et al., 2013), but are not optimised to approximate well the non-linear and site-specific relationships that govern soil water deficits, in particular they neglect the soil-specific water retention characteristics (Wang et al., 2015). Some soils retain water better than others, for example sandy clay loam in Bourke may retain more water than sandy loam in Cairns or Melbourne (Wong et al., 2016), and affect the number, depth and timing of periods of soil water shortage. As numerous drought indices have been developed, some of which incorporate additional variables beyond rainfall and potential evaporation, there is scope to explore alternatives (Mpelasoka et al., 2008). However, notwithstanding the limited scope of this paper, our results are in accordance with other findings, for example, in North Carolina where the SPI can be used to represent soil moisture variation (Asadi Zarch et al., 2015; Khalili et al., 2011).

We averaged the climate data over three months before they were used for the monthly SPI and RDI calculation (Eqs. (1) and (2a), (2b)), whereas the simulation used a daily time step. The performance was potentially limited by this discrepancy in time scales. For example, for the shallow soil, there were cases where three simulated soil moisture minima were contained within one long drought event identified by the index, while in other cases the simulated event was too short to be recognised by the more dampened response

of the index. Results show a poorer correlation between the indices and standardised soil water pressure if a 12-monthly averaged period was used instead (with the exception of Melbourne (Appendix D)). In cases, higher correlations have been observed using the SPI with an averaging period less than three months especially for the top 10 cm of soil (Sims and Raman, 2002), although longer timescales have been recommended in general for drought analysis (Du et al., 2013). Contrasting conclusions about the optimal averaging period may be explained by differences in climate, soil and water management contexts (Vicente-Serrano et al., 2012; Xu et al., 2012). A 12-monthly timescale may not capture the significance of the five to six-monthly wet and dry cycle such as in Cairns; and a three-monthly timescale may not capture the annual lag-times of groundwater-fed irrigation schemes. Thus, it is a matter of finding the suitable timescale for each specific context, and it may be helpful to present results for alternative time-scales (Vicente-Serrano et al., 2012).

Given the more rapid variations in soil water content experienced in the shallow soil (represented by the 0–5 cm depth range), if drought indices are used as a planning tool for initial plant establishment, a shorter time scale than three months is likely to be preferred (correlations between standardised soil water pressure and drought index values for the one-month time scale are shown in Appendix D). Generally, the soil water model performed better for shallow soils than for deeper soils as FR*-FR for deep soils is always higher than FR*-FR of shallow soils (except for the shallow soil in Melbourne) (Fig. 6). We presume this is because it operates on a daily time-step as opposed to the three-monthly averages used by the drought indices and therefore, despite its uncertainty, performs relatively well for short-term and near-surface periods of limited soil water availability.

We opted to use the monthly minimum rather than the monthly average soil water pressure. Although using the average may have provided a stronger correlation between the drought indices and the Hydrus-1D outputs, we selected the minimum based on the assumption that one incidence of exceeding a species-specific water pressure threshold causes irreversible plant water stress (Blum, 2011). This reference point is more biologically relevant than monthly averaged soil water pressure. Further, we opted to use soil water pressure over soil moisture because it would allow examination of potential water fluxes between plant roots and the soil water storage. Also due to the monotonic behaviour of water retention curve, use of soil moisture over soil water pressure should not affect the findings on the false alarm (FAR) and failure rate (FR). Hence, although soil moisture is a valuable metric defining the total store of subsurface water, the soil water pressure provides the relevant information required to assess water availability for plants.

The performances of the indices reported in this paper are conditional on the accuracy of the soil model Hydrus-1D. Although an uncertainty analysis was performed, this only involved arbitrary one-at-a-time perturbations to soil hydraulic property parameters, and did not explicitly examine the sensitivity of performance to structural errors in Hydrus-1D such as effects of anisotropy and heterogeneity of soil properties, the spatial-temporal distribution of plant water uptake, and the applied lower and upper boundary conditions. These errors may influence how the performances varied between the SPI and RDI, between the two depths and over the three selected sites. A potential approach to extending the uncertainty analysis would be a Monte Carlo based global sensitivity analysis, as well as exploring some of the structural uncertainties such as the single porosity assumption, the potential evaporation model and boundary condition assumptions (Le Vine et al., 2016). This would likely support the result that the drought indices are more robust predictors of soil moisture drought than using a default model such as our application of Hydrus-1D, and it would also identify the priority uncertainties.

A particularly interesting result was that the SPI performed considerably better than the RDI (Fig. 5). Overall, the SPI performed better than the RDI (except for pF^5 at Bourke), illustrating that in general the inclusion of potential evaporation in the RDI confounds the prediction of drought for these sites, although this result may be affected by potential evaporation and Hydrus model errors as discussed above. For arid Bourke, there was less benefit using the SPI over the RDI (Fig. 5), which we speculate is due to a stronger and more linear influence of potential evaporation on the soil moisture minima at that site (Asadi Zarch et al., 2015; Khalili et al., 2011). The differences in the correlations shown in Fig. 5 are consistent with the differences seen in FR and FAR values (Table 3), with both showing that the better predictor of droughts is the SPI.

The rationale behind using the 75th percentile threshold for soil water pressure is that a physically based value cannot be usefully determined. Rather, it is assumed that native plants have been established over long periods and are adapted to the local environmental conditions and would suffer similar levels of water stress at the 75th percentile soil water pressure across the three locations. Of course this implies different absolute quantities of soil water pressure. For example, the 75th percentile corresponds to pF 3.4 in Bourke, but is only pF 2.3 and 2.1 in Melbourne and Cairns, respectively. In order to address the issue of an arbitrarily selected threshold, we tested our methods within the range of 45–95% (Fig. 3).

Ideally, indices such as the SPI or RDI should be compared with empirical field data. However, such empirical data are often not available (such as in our study locations), primarily due to the cost- and time-intensive nature of long-term monitoring programs. As a solution remotely sensed soil moisture data are increasingly available, but are expensive, cover only the last two decades, and shallow soil layers have limited accuracy (Dorigo et al., 2010; Houser et al., 1998; Mishra et al., 2015). For example complex land-surface models have been used to infer long-term soil moisture data by demonstrating the limited availability of long-term empirical soil moisture data to test the capability of drought indices to detect soil moisture droughts (Cammalleri et al., 2016). This encourages the approach of using empirically derived soil water retention curves and a physically based soil water model as a reference or control scenarios is a valuable alternative. Hence, a logical step before implementing any long-term campaigns is to test their feasibility in a pilot study, for example, using physically based models such as Hydrus-1D with available empirical data such as rainfall and evaporation and soil water retention characteristics, as demonstrated in our work. However, numerical models are simple representation of physical processes and would have limited predictive power and the model uncertainty addressed in this study is a common

Table 4
Merits of the alternative approaches to detect soil moisture droughts.

	Drought indices		Standardised soil water pressure
	SPI	RDI	
Data requirement	rainfall	rainfall, potential evaporation	rainfall, irrigation, potential evaporation, soil type and soil hydraulic parameters
Time for data/model preparation	low	low	high
Calculation time	low	low	moderate
Cost for data	mostly free	sometimes have to purchase	may be expensive for some locations
Data availability	available for most locations	available for some locations	restricted to few locations or have to measure in sites
Applicability to any climatic region	have issues with arid regions	can apply to any climate	can apply to any climate
Applicability to future climate	accounts for changes in precipitation	accounts for changes in precipitation and potential evaporation	accounts for changes in precipitation, potential evaporation and soil hydraulic properties

practice in the environmental modelling literature (Muleta and Nicklow, 2005; Uusitalo et al., 2015).

Table 4 summarises the comparison of the merits of drought indices versus physically based soil water models for soil water drought estimation. The SPI and RDI require only meteorological data, which are often freely available, although they are less often available for the recommended minimum period of 30 years (McKee et al., 1993), and accuracy may be poor if the location of interest is far from a rain gauge. Data preparation and estimation of the drought index is easy to follow and not time consuming (McKee et al., 1993; Tsakiris et al., 2007). However, the drought index only gives the anomaly from the average value, rather than a value that is physically meaningful. For an example the same drought index value for two different sites will show different soil water pressures, e.g. for an SPI value of -2, the corresponding soil water pressure (hPa) is -37.32 for Cairns and -2381.7 for Bourke.

Another limitation of the approach taken here is the limited length of climate time series. We used historic rainfall and potential evaporation data for 25 years, which represents only a limited range of drought extremes, and ideally longer-term data would be used. The use of monthly standardised soil water pressure minima provided 300 samples for the assessment of performance, however clearly these samples are not independent droughts and a more statistically robust assessment would be based on annual minima, if enough samples (long enough time series) could be obtained.

5. Conclusions

The study reveals that the selected simple drought indices, SPI and RDI, perform better than the physically based soil water model over three soil types and climates in Eastern Australia. This was based on comparing the failure rate (FR) and false alarm rate (FAR), measures of how reliably the indices detected simulated soil water drought events. Generally, SPI performed better than RDI, potentially due to the over-simple treatment of potential evaporation reducing the correlation between the RDI and standardised soil water pressure values, as well as the dominant effect of precipitation for the climates and soils considered. Also the study has highlighted the influence of drought index time scale, with a three month climate aggregation period giving overall the best results. However, exceptions exist with respect to both the best index and the best time scale. Finally the physically based simulation model is unlikely to be more useful than the SPI for soil water drought estimation due to uncertainty in the soil water retention curves, which are generalised for the soil classes rather than based on local calibration. We conclude that local calibration of soil hydraulic parameters is a prerequisite for preferring such models over simple indices.

Conflict of interest

The authors declare that they have no conflict of interest.

Acknowledgements

This study was made possible by the International Postgraduate Research Scholarship and Australian Postgraduate Award awarded to D. Halwatura.

Appendix A. Configuration of the Hydrus-1D model for all selected sites

Table A1

Table A1
Configuration of the Hydrus-1D model for all selected sites.

Attribute	Value
Soil Profile	
Depth (mm)	50 mm or 300 mm
No. of layers	1
No. of nodes	100
Nodal density	100 (upper), 1 (lower)
Hydraulic model and boundary conditions	
Single Porosity model	Van Genuchten-Mualem
Hysteresis	No hysteresis was included
Upper boundary	Atmospheric (rainfall and potential evaporation data) with surface runoff
Lower boundary	Free drainage
Iteration criteria and time information	
Maximum No. of iterations	10
Water content tolerance	10^{-5}
Pressure head tolerance (mm)	1
Lower [upper] optimal iteration range	3 [7]
Lower [upper] time step multiplication factor	1.3 [0.7]
Lower [upper] limit of the tension interval (mm)	10^{-5} [10^{6}]
Initial [final] time (day)	0 [9125]
Initial time step (day)	10^{-3}
Minimum [maximum] time step (day)	10^{-5} [1]

Appendix B. Conceptual schematics of applied methods

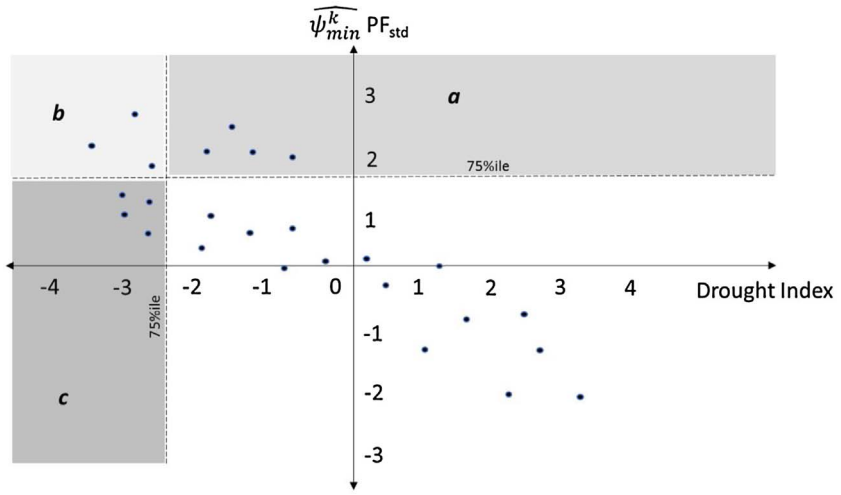

Fig. B1. Conceptual schematic to assist with interpretation of the failure rate (FR) and false alarm rate (FAR) values. The threshold values (dashed lines) divide the possible pairs of values [drought index, monthly minimum standardised soil water pressure] into four segments, upon which the calculations of FR and FAR are based (Section 2, step 3). The segments (a, b, c) represent the low soil water pressure events that are not (a) or are (b) detected by the drought index, and the drought events detected by the drought index that do not (c) correspond to periods of low soil water pressure.

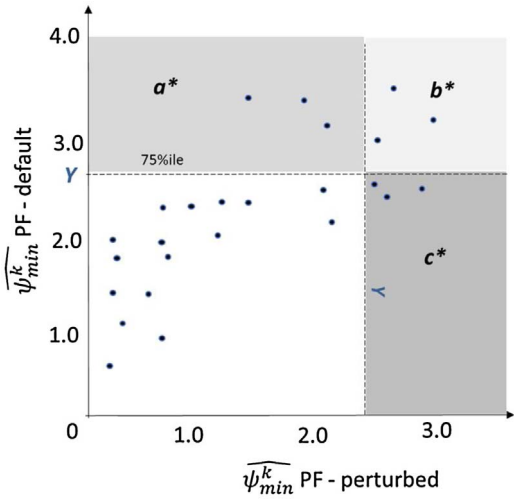

Fig. B2. Conceptual schematic to assist with interpretation of the failure rate (FR*) and false alarm rate (FAR*) values. The threshold values (dashed lines) divide the possible pairs of values [monthly minimum standardised soil water pressure, perturbed monthly minimum standardised soil water pressure] into four segments, upon which the calculations of FR* and FAR* are based (Eqs. (7) and (8)). The segments (a–c) represent the drought events simulated by the default model that are not (a) or are (b) detected by the perturbed model, and the drought events simulated by the perturbed model that do not (c) correspond to those simulated by the default model.

Appendix C. Normalised relative sensitivity S of simulated soil water pressure to uncertainty in the water retention curves

Table C1

Table C1
Normalised relative sensitivity S (Eq. (6)) of simulated soil water pressure to uncertainty in parameters of the water retention curve. Values in blue-bold and green-italics are the highest and the median values of percentage change, respectively, over all 10 perturbations.

Site and the soil profile	Assessing parameter	Percentage of change in the parameter									
		50%-	40%-	%30-	20%-	10%-	10%+	20%+	30%+	40%+	50%+
Bourke 5 cm	θr 0.07	0.38	**0.97**	0.57	0.58	0.84	***0.44***	0.15	0.06	0.02	0.01
	θs 0.33	0.36	**1.02**	0.55	0.55	0.77	***0.36***	0.11	0.03	0.00	0.02
	α 0.02	0.36	**0.95**	0.54	0.53	0.74	***0.33***	0.09	0.02	0.01	0.03
	n 1.30	NA	NA	NA	NA	**2.45**	2.34	***0.94***	0.54	0.36	0.26
Bourke 30 cm	θr 0.07	0.50	0.66	0.70	0.90	**1.57**	1.24	***0.56***	0.33	0.23	0.16
	θs 0.33	0.49	0.67	0.69	0.87	**1.51**	1.18	***0.52***	0.31	0.21	0.15
	α 0.02	0.50	0.67	0.68	0.85	**1.47**	1.13	***0.50***	0.29	0.19	0.14
	n 1.30	NA	NA	NA	NA	**2.69**	2.36	***1.06***	0.65	0.45	0.34
Cairns 5 cm	θr 0.05	1.14	0.63	2.50	3.51	***2.26***	**3.75**	2.85	0.65	0.23	1.37
	θs 0.47	1.10	0.56	2.50	3.51	***2.18***	**4.02**	2.82	0.62	0.20	1.36
	α 0.19	1.12	0.61	2.46	3.45	***2.18***	**3.61**	2.79	0.61	0.18	1.35
	n 1.21	NA	NA	NA	NA	NA	**2.86**	3.22	***2.03***	0.73	0.40
Cairns 30 cm	θr 0.05	NA	NA	NA	2.77	**3.33**	2.24	***1.42***	0.73	0.42	NA
	θs 0.47	NA	NA	NA	2.39	**2.85**	***2.16***	1.47	0.72	0.40	NA
	α 0.19	0.24	0.35	0.81	2.60	**3.20**	2.14	***1.37***	NA	NA	NA
	n 1.21	NA	NA	NA	NA	NA	**1.44**	0.51	1.06	***0.74***	0.46
Melbourne 5 cm	θr 0.10	0.08	0.03	0.16	0.37	**0.96**	0.11	***0.25***	0.27	0.26	0.24
	θs 0.51	0.06	0.05	0.19	0.42	**1.07**	0.34	0.21	***0.26***	0.26	0.25
	α 0.11	0.06	0.07	0.21	0.46	**1.14**	0.06	0.34	0.32	***0.30***	0.27
	n 1.37	NA	NA	NA	0.33	**0.30**	***0.16***	0.16	0.16	0.22	0.07
Melbourne 30 cm	θr 0.10	0.08	0.13	0.19	0.32	0.70	**0.74**	0.38	***0.28***	0.22	0.19
	θs 0.51	0.08	0.13	0.20	0.34	0.74	**0.74**	0.40	***0.29***	0.23	0.20
	α 0.11	0.08	0.14	0.22	0.36	0.80	**0.86**	0.45	***0.32***	0.26	0.22
	n 1.37	NA	NA	NA	NA	0.35	**0.45**	***0.25***	0.18	0.14	0.10

Appendix D

Fig. D1

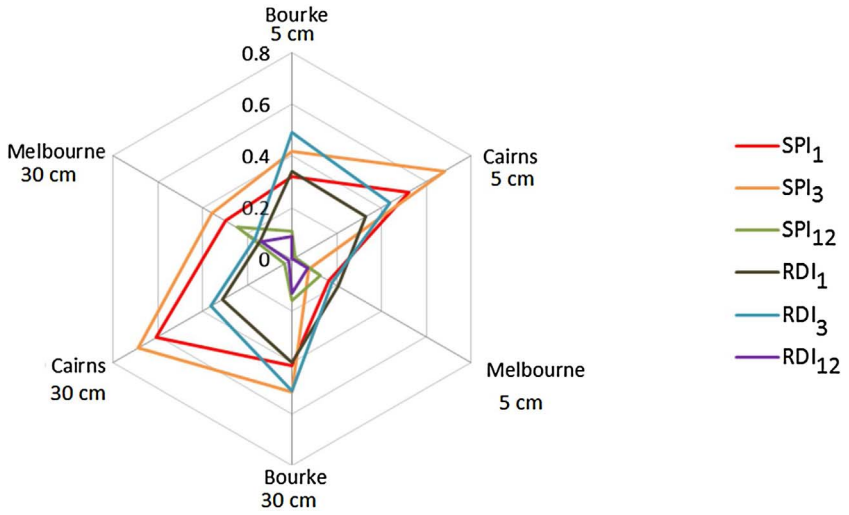

Fig. D1. Correlations between simulated monthly minimum soil water pressure (pF) and the SPI and RDI for 5 cm and 30 cm soil profile at a one-, three- and 12-monthly timescale, respectively.

Appendix E

Fig. E1

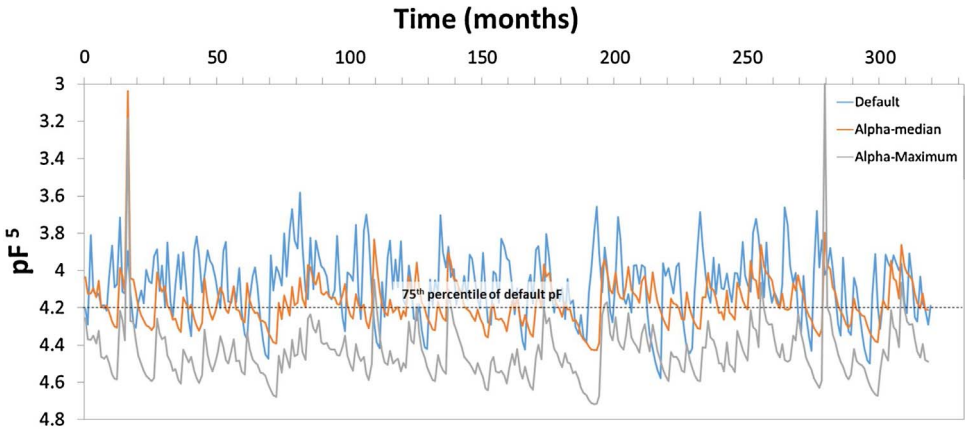

Fig. E1. Default and perturbed (median and maximums for parameter alpha) monthly minimum soil water pressure in 5 cm depth for Bourke.

References

Agnew, C., 2000. Using the SPI to Identify Drought. Winter 1999–Spring 2000. University College London, London, United Kingdom.
American Meteorological Society, 1997. Meteorological drought—Policy statement. Bull. Am. Meteorol. Soc. 78, 847–849.
Anderson, W., et al., 2012. Towards an integrated soil moisture drought monitor for East Africa. Hydrol. Earth Syst. Sci. 16 (8), 2893–2913.
Asadi Zarch, M.A., Sivakumar, B., Sharma, A., 2015. Droughts in a warming climate: a global assessment of Standardized Precipitation Index (SPI) and Reconnaissance Drought Index (RDI). J. Hydrol. 526, 183–195. http://dx.doi.org/10.1016/j.jhydrol.2014.09.071.
Australian Soil Resource Information System, 2011. Australian Soil Resource Information System. CSIRO Land and Water.
Barua, S., Perera, B.J.C., Ng, A.W.M., 2009. A comparative drought assessment of yarra river catchment in Victoria, Australia. In: 18th World Imacs Congress and Modsim09 International Congress on Modelling and Simulation: Interfacing Modelling and Simulation with Mathematical and Computational Sciences. Univ Western Australia, Nedlands. pp. 3245–3251.
Blum, A., 2011. Plant Water Relations, Plant Stress and Plant Production. Springer.
Bond, B.J., Kavanagh, K.L., 1999. Stomatal behavior of four woody species in relation to leaf-specific hydraulic conductance and threshold water potential. Tree

Physiol. 19 (8), 503–510.
Bureau of Meteorology: Climate data, http://www.bom.gov.au/ climate/data/, last access: April 2013.
Cammalleri, C., Micale, F., Vogt, J., 2016. A novel soil moisture-based drought severity index (DSI) combining water deficit magnitude and frequency. Hydrol. Process. 30 (2), 289–301.
Carrão, H., Russo, S., Sepulcre-Canto, G., Barbosa, P., 2016. An empirical standardized soil moisture index for agricultural drought assessment from remotely sensed data. Int. J. Appl. Earth Observ. Geoinf. 48, 74–84. http://dx.doi.org/10.1016/j.jag.2015.06.011.
Carrick, P.J., Krüger, R., 2007. Restoring degraded landscapes in lowland Namaqualand: lessons from the mining experience and from regional ecological dynamics. J. Arid Environ. 70 (4), 767–781. http://dx.doi.org/10.1016/j.jaridenv.2006.08.006.
Chen, M., Willgoose, G.R., Saco, P.M., 2014. Spatial prediction of temporal soil moisture dynamics using HYDRUS-1D. Hydrol. Process. 28 (2), 171–185.
Chowdhary, H., Singh, V.P., 2010. Reducing uncertainty in estimates of frequency distribution parameters using composite likelihood approach and copula-based bivariate distributions. Water Resour. Res. 46 (11).
Dai, A.G., 2012. Drought under global warming: a review. Wiley Interdiscip. Rev.–Clim. Change 3 (6), 617.
Dorigo, W., et al., 2010. Error characterisation of global active and passive microwave soil moisture datasets. Hydrol. Earth Syst. Sci. 14 (12), 2605–2616.
Du, J., Fang, J., Xu, W., Shi, P.J., 2013. Analysis of dry/wet conditions using the standardized precipitation index and its potential usefulness for drought/flood monitoring in Hunan Province, China. Stoch. Environ. Res. Risk Assess. 27 (2), 377–387. http://dx.doi.org/10.1007/s00477-012-0589-6.
Edwards, D.C., 1997. Characteristics of 20th Century Drought in the United States at Multiple Time Scales, DTIC, Document. Air force institute of tech wright-patterson, AFB, OH.
Elkollaly, M., Khadr, M., Zeidan, B., 2017. Drought analysis in the Eastern Nile basin using the standardized precipitation index. Environ. Sci. Pollut. Res. 1–15. http://dx.doi.org/10.1007/s11356-016-8347-9.
Granier, A., Bréda, N., Biron, P., Villette, S., 1999. A lumped water balance model to evaluate duration and intensity of drought constraints in forest stands. Ecol. Model. 116 (2), 269–283.
Gupta, M., Srivastava, P.K., Islam, T., Bin Ishak, A.M., 2014. Evaluation of TRMM rainfall for soil moisture prediction in a subtropical climate. Environ. Earth Sci. 71 (10), 4421–4431. http://dx.doi.org/10.1007/s12665-013-2837-6.
Halwatura, D., Lechner, A.M., Arnold, S., 2015a. Drought severity-duration-frequency curves: a foundation for risk assessment and planning tool for ecosystem establishment in post-mining landscapes. Hydrol. Earth Syst. Sci. 19 (2), 1069–1091. http://dx.doi.org/10.5194/hess-19-1069-2015.
Halwatura, D.H., McIntyre, N., Lechner, A., Arnold, S., 2015b. Adequacy of simple agricultural drought indices. In: Second International Conference on Agriculture, Aquaculture and Animal Science. International Center for Research & Development., Colobmo, Sri Lanka. pp. 30–36.
Halwatura, D., McIntyre, N., Lechner, A.M., Arnold, S., 2016. Reliability of meteorological drought indices for predicting soil moisture droughts. Hydrol. Earth Syst. Sci. Discuss. http://dx.doi.org/10.5194/hess-2016-467.
Hao, Z., AghaKouchak, A., 2013. Multivariate standardized drought index: a parametric multi-index model. Adv. Water Resour. 57 (0), 12–18. http://dx.doi.org/10.1016/j.advwatres.2013.03.009.
Hao, Z., et al., 2016. A theoretical drought classification method for the multivariate drought index based on distribution properties of standardized drought indices. Adv. Water Resour. 92, 240–247. http://dx.doi.org/10.1016/j.advwatres.2016.04.010.
Hollander, H.M., Wang, Z.J., Assefa, K.A., Woodbury, A.D., 2016. Improved recharge estimation from portable, low-cost weather stations. Groundwater 54 (2), 243–254. http://dx.doi.org/10.1111/gwat.12346.
Houser, P.R., et al., 1998. Integration of Soil Moisture Remote Sensing and Hydrologic Modeling Using Data Assimilation. http://dx.doi.org/10.1029/1998wr900001.
Jamshidi, H., Khalili, D., Zadeh, M.R., Hosseinipour, E.Z., 2011. Assessment and Comparison of SPI and RDI Meteorological Drought Indices in Selected Synoptic Stations of Iran. pp. 1161–1173.
Köppen, W., 1936. Das geographisca System der Klimate. In: Köppen, W., Geiger, G. (Eds.), Handbuch der Klimatologie, Handbuch der Klimatologie, vol. 1: C. Gebr, Borntraeger.
Kato, C., Nishimura, T., Imoto, H., Miyazaki, T., 2010. Applicability of HYDRUS to predict soil moisture and temperature in vadose zone of arable land under monsoonal climate region, Tokyo.
Keyantash, J., Dracup, J.A., 2002. The quantification of drought: an evaluation of drought indices. Bull. Am. Meteorol. Soc. 83 (8), 1167–1180. http://dx.doi.org/10.1175/1520-0477(2002)083<1191:TQODAE>2.3.CO;2.
Khalili, D., Farnoud, T., Jamshidi, H., Kamgar-Haghighi, A.A., Zand-Parsa, S., 2011. Comparability analyses of the SPI and RDI meteorological drought indices in different climatic zones. Water Resour. Manag. 25 (6), 1737–1757.
Khedun, C.P., Chowdhary, H., Mishra, A.K., Giardino, J.R., Singh, V.P., 2012. Water deficit duration and severity analysis based on runoff derived from Noah Land Surface Model. J. Hydrol. Eng. 18 (7), 817–833.
Kirono, D., Kent, D., Hennessy, K., Mpelasoka, F., 2011. Characteristics of Australian droughts under enhanced greenhouse conditions: results from 14 global climate models. J. Arid Environ. 75 (6), 566–575.
Kostopoulou, E., Giannakopoulos, C., Krapsiti, D., Karali, A., 2017. Temporal and spatial trends of the standardized precipitation index (SPI) in Greece using observations and output from regional climate models. In: Karacostas, T., Bais, A., Nastos, P.T. (Eds.), Perspectives on Atmospheric Sciences. Springer International Publishing, Cham, pp. 475–481. http://dx.doi.org/10.1007/978-3-319-35095-0_68.
Kumar, R., Jude, L.M., Van Loon Anne, F., Teuling Adriaan, J., Barthel, Roland, Ten Broek, Jurriaan, Mai, Juliane, Samaniego, Luis, Attinger, Sabine, 2016. Multiscale evaluation of the standardized precipitation index as a groundwater drought indicator. Hydrol. Earth Syst. Sci. 20 (3), 1117.
Kwak, J., et al., 2015. Impact of climate change on hydrological droughts in the upper Namhan River basin, Korea. KSCE J. Civ. Eng. 19 (2), 376–384.
Le Vine, N., Butler, A., McIntyre, N., Jackson, C., 2016. Diagnosing hydrological limitations of a land surface model: application of JULES to a deep-groundwater chalk basin. Hydrol. Earth Syst. Sci. 20 (1), 143–159.
Li, H., Robock, A., Liu, S., Mo, X., Viterbo, P., 2005. Evaluation of reanalysis soil moisture simulations using updated Chinese soil moisture observations. J. Hydrometeorol. 6 (2), 180–193. http://dx.doi.org/10.1175/JHM416.1.
Ma'rufah, U., Hidayat, R., Prasasti, I., 2017. Analysis of relationship between meteorological and agricultural drought using standardized precipitation index and vegetation health index. In: IOP Conference Series: Earth and Environmental Science. Vol. 54. No. 1. IOP Publishing.
Martínez-Fernández, J., Ceballos, A., Casado, S., Morán, C., Hernández, V., 2005. Runoff and Soil Moisture Relationships in a Small Forested Basin in the Sistema Central Ranges (Spain). IAHS-AISH Publicationpp. 31–36.
Martínez-Fernández, J., González-Zamora, A., Sánchez, N., Gumuzzio, A., 2015. A soil water based index as a suitable agricultural drought indicator. J. Hydrol. 522, 265–273. http://dx.doi.org/10.1016/j.jhydrol.2014.12.051.
McCarthy, J.J., 2001. Climate Change 2001: Impacts, Adaptation, and Vulnerability: Contribution of Working Group II to the Third Assessment Report of the Intergovernmental Panel on Climate Change. Cambridge University Press.
McKee, T.B., Doesken, N.J., Kleist, John, 1993. The relationship of drought frequency and duration to time scales. In: Proceedings of the 8th Conference on Applied Climatology. American Meteorological Society Boston, MA, Anaheim California. pp. 179–183.
Mishra, A.K., Singh, V.P., 2011. Drought modelling –a review. J. Hydrol. 403 157–175.
Mishra, A.K., et al., 2015. Anatomy of a local-scale drought: application of assimilated remote sensing products, crop model, and statistical methods to an agricultural drought study. J. Hydrol. 526, 15–29.
Mpelasoka, F., Hennessy, K., Jones, R., Bates, B., 2008. Comparison of suitable drought indices for climate change impacts assessment over Australia towards resource management. Int. J. Climatol. 28 (10), 1283–1292. http://dx.doi.org/10.1002/joc.1649.
Mueller, B., Zhang, X., 2016. Causes of drying trends in northern hemispheric land areas in reconstructed soil moisture data. Clim. Change 134 (1), 255–267. http://dx.doi.org/10.1007/s10584-015-1499-7.
Muleta, M.K., Nicklow, J.W., 2005. Sensitivity and uncertainty analysis coupled with automatic calibration for a distributed watershed model. J. Hydrol. 306 (1–4), 127–145. http://dx.doi.org/10.1016/j.jhydrol.2004.09.005.
National Drought Mitigation Center, 2013. Drought Measurements.

Naylor, S., Letsinger, S.L., Ficklin, D.L., Ellett, K.M., Olyphant, G.A., 2016. A hydropedological approach to quantifying groundwater recharge in various glacial settings of the mid-continental USA. Hydrol. Process. 30 (10), 1594–1608. http://dx.doi.org/10.1002/hyp.10718.
Oakley, J.E., O'Hagan, A., 2004. Probabilistic sensitivity analysis of complex models: a Bayesian approach. J. R. Stat. Soc.: Ser. B (Stat. Methodol.) 66 (3), 751–769.
Palmer, W.C., 1965. Meteorological Drought. Research Paper No. 45. US Department of Commerce. Weather Bureau, Washington, DC.
Palmer, W.C., 1968. Keeping Track of Crop Moisture Conditions, Nationwide: The New Crop Moisture Index.
Palmer, W.C., 1969. Crop production estimates and palmer crop moisture index. Bull. Am. Meteorol. Soc. 50 (6) 468- & .
Pan, F., Pachepsky, Y.A., Guber, A.K., Hill, R.L., 2011. Information and complexity measures applied to observed and simulated soil moisture time series. Hydrol. Sci. J. 56 (6), 1027–1039. http://dx.doi.org/10.1080/02626667.2011.595374.
Passioura, J., 2007. The drought environment: physical, biological and agricultural perspectives. J. Exp. Bot. 58 (2), 113–117.
Peel, M.C., Finlayson, B.L., McMahon, T.A., 2007. Updated world map of the Köppen-Geiger climate classification. Hydrol. Earth Syst. Sci. 11 (5), 1633–1644. http://dx.doi.org/10.5194/hess-11-1633-2007.
Prentice, I.C., et al., 1992. Special Paper: a global biome model based on plant physiology and dominance, soil properties and climate. J. Biogeogr. 19 (2), 117–134. http://dx.doi.org/10.2307/2845499.
Quiring, S.M., 2009. Monitoring drought: an evaluation of meteorological drought indices. Geogr. Compass 3 (1), 64–88. http://dx.doi.org/10.1111/j.1749-8198.2008.00207.x.
Rahmat, S.N., Jayasuriya, N., Bhuiyan, M., 2015. Assessing droughts using meteorological drought indices in Victoria, Australia. Hydrol. Res. 46 (3), 463–476. http://dx.doi.org/10.2166/nh.2014.105.
Rodriguez-Iturbe, I., 2000. Ecohydrology: a hydrologic perspective of climate-soil-vegetation dynamies. Water Resour. Res. 36 (1), 3–9.
Saghafian, B., Shokoohi, Alireza, Raziei, T., 2003. severity duration-frequency curves for an arid region. Hydrol. Mediterr. Semiarid Reg. 305–311.
Schwarzel, K., Simunek, J., van Genuchten, M.T., Wessolek, G., 2006. Measurement and modeling of soil-water dynamics and evapotranspiration of drained peatland soils. J. Plant Nutr. Soil Sci. 169 (6), 762–774. http://dx.doi.org/10.1002/jpln.200621992.
She, D., Mishra, A.K., Xia, J., Zhang, L., Zhang, X., 2016. Wet and dry spell analysis using copulas. Int. J. Climatol. 36 (1), 476–491.
Sheffield, J., Wood, E.F., Roderick, M.L., 2012. Little change in global drought over the past 60 years. Nature 491 (7424), 435–438. http://www.nature.com/nature/journal/v491/n7424/abs/nature11575html#supplementary-information.
Shiau, J.T., Modarres, R., 2009. Copula-based drought severity-duration-frequency analysis in Iran. Meteorol. Appl. 16 (4), 481–489. http://dx.doi.org/10.1002/met.145.
Shiau, J.-T., Modarres, R., Nadarajah, S., 2012. Assessing multi-site drought connections in Iran using empirical Copula. Environ. Model. Assess. 17 (5), 469–482. http://dx.doi.org/10.1007/s10666-012-9318-2.
Shiau, J.T., 2006. Fitting drought duration and severity with two-dimensional Copulas. Water Resour. Manag. 20, 795–815.
Shokoohi, A., Morovati, R., 2015. Basinwide comparison of RDI and SPI within an IWRM framework. Water Resour. Manag. 29 (6), 2011–2026. http://dx.doi.org/10.1007/s11269-015-0925-y.
Sims, A.P., Raman, S., 2002. Adopting drought indices for estimating soil moisture: a North Carolina case study. Geophys. Res. Lett. 29 (8).
Šimůnek, J., van Genuchten, M.T., Šejna, M., 2008. Development and applications of the HYDRUS and STANMOD software packages and related codes. Vadose Zone J. 7 (2), 587–600. http://dx.doi.org/10.2136/vzj2007.0077.
Šimůnek, J., van Genuchten, M.T., Šejna, M., 2016. Recent developments and applications of the HYDRUS computer software packages. Vadose Zone J. 15 (7).
Svoboda, M., et al., 2002. The drought monitor. Bull. Am. Meteorol. Soc. 83 (8).
Törnros, T., Menzel, L., 2014. Addressing drought conditions under current and future climates in the Jordan River region. Hydrol. Earth Syst. Sci. 18 (1), 305–318.
Tezara, W., Mitchell, V., Driscoll, S., Lawlor, D., 1999. Water stress inhibits plant photosynthesis by decreasing coupling factor and ATP. Nature 401 (6756), 914–917.
Touchan, R., Funkhouser, G., Hughes, M.K., Erkan, N., 2005. Standardized precipitation index reconstructed from Turkish tree-ring widths. Clim. Change 72 (3), 339–353.
Tsakiris, G., Vangelis, H., 2005. Establishing a Drought Index Incorporating Evapotranspiration European Water, vol. 9/10. pp. 3–11.
Tsakiris, G., Pangalou, D., Vangelis, H., 2007. Regional drought assessment based on the Reconnaissance Drought Index (RDI). Water Resour. Manag. 21, 821–833.
UNEP, U.N.E.P., 1992. World Atlas of Desertification, London.
United States Drought Monitor, 2017. Drought Severity Classification. The National Drought Mitigation Center, University of Nebraska-Lincoln.
Uusitalo, L., Lehikoinen, A., Helle, I., Myrberg, K., 2015. An overview of methods to evaluate uncertainty of deterministic models in decision support. Environ. Model. Softw. 63, 24–31. http://dx.doi.org/10.1016/j.envsoft.2014.09.017.
Van Genuchten, M.T., Leij, F., Yates, S., 1991. The RETC Code for Quantifying the Hydraulic Functions of Unsaturated Soils. Robert S. Kerr Environmental Research Laboratory.
Van Loon, A.F., et al., 2016. Drought in a human-modified world: reframing drought definitions, understanding, and analysis approaches. Hydrol. Earth Syst. Sci. 20 (9), 3631–3650. http://dx.doi.org/10.5194/hess-20-3631-2016.
Vangelis, H., Tigkas, D., Tsakiris, G., 2013. The effect of PET method on Reconnaissance Drought Index (RDI) calculation. J. Arid Environ. 88 (0), 130–140. http://dx.doi.org/10.1016/j.jaridenv.2012.07.020.
Vicente-Serrano, S.M., et al., 2012. Performance of drought indices for ecological agricultural, and hydrological applications. Earth Interact. 16 (10), 1–27. http://dx.doi.org/10.1175/2012EI000434.1.
Wang, A., Lettenmaier, D.P., Sheffield, J., 2011. Soil moisture drought in China, 1950–2006. J. Clim. 24 (13), 3257–3271.
Wang, H., Rogers, J.C., Munroe, D.K., 2015. Commonly used drought indices as indicators of soil moisture in China. J. Hydrometeorol. 16 (3), 1397–1408. http://dx.doi.org/10.1175/JHM-D-14-0076.1.
Wang, H., et al., 2016. Monitoring winter wheat drought threat in Northern China using multiple climate-based drought indices and soil moisture during 2000–2013. Agric. Forest Meteorol. 228–229, 1–12. http://dx.doi.org/10.1016/j.agrformet.2016.06.004.
Wilson, T.B., et al., 2016. Site-specific soil properties of the US climate reference network soil moisture. Vadose Zone J. 15 (11).
Wong, J.T.F., Chen, Z., Chen, X., Ng, C.W.W., Wong, M.H., 2016. Soil-water retention behavior of compacted biochar-amended clay: a novel landfill final cover material. J. Soils Sediments 1–9.
Wonkka, C.L., Twidwell, D., Franz, T.E., Taylor, C.A., Rogers, W.E., 2016. Persistence of a severe drought increases desertification but not woody dieback in semiarid savanna. Rangel. Ecol. Manag. 69 (6), 491–498.
Xu, Q., et al., 2012. Effects of rainfall on soil moisture and water movement in a subalpine dark coniferous forest in southwestern China. Hydrol. Process. 26 (25), 3800–3809. http://dx.doi.org/10.1002/hyp.8400.
Yagci, A.L., Di, L., Deng, M., 2013. The effect of land-cover change on vegetation greenness-based satellite agricultural drought indicators: a case study in the southwest climate division of Indiana, USA. Int. J. Remote Sens. 34 (20), 6947–6968. http://dx.doi.org/10.1080/01431161.2013.810824.
Zarei, A.R., Moghimi, M.M., Mahmoudi, M.R., 2016. Analysis of changes in spatial pattern of drought using RDI index in south of Iran. Water Resour. Manag. 30 (11), 3723–3743. http://dx.doi.org/10.1007/s11269-016-1380-0.
Zargar, A., Sadiq, R., Naser, B., Khan, F.I., 2011. A review of drought indices. Environ. Rev. 19, 333–349.
Zawadzki, J., Kędzior, M., 2016. Soil moisture variability over Odra watershed: comparison between SMOS and GLDAS data. Int. J. Appl. Earth Obs. Geoinf. 45 (Part B), 110–124. http://dx.doi.org/10.1016/j.jag.2015.03.005.
Zhang, L., Jiao, W., Zhang, H., Huang, C., Tong, Q., 2017. Studying drought phenomena in the Continental United States in 2011 and 2012 using various drought indices. Remote Sens. Environ. 190, 96–106. http://dx.doi.org/10.1016/j.rse.2016.12.010.
Zhu, Y.H., et al., 2009. Simulation of Populus euphratica root uptake of groundwater in an arid woodland of the Ejina Basin. China. Hydrol. Process. 23 (17), 2460–2469. http://dx.doi.org/10.1002/hyp.7353.